

# Giant Skyrmions Stabilized by Dipole-Dipole Interactions in Thin Ferromagnetic Films

Motohiko Ezawa  
(Dated: October 8, 2018)

Motivated by a recent magnetization reversal experiment on a TbFeCo thin film, we study a topological excitation in the anisotropic nonlinear sigma model together with the Zeeman and magnetic dipole-dipole interactions. Dipole-dipole interactions turn a ferromagnet into a frustrated spin system, which allows a nontrivial spin texture such as a giant skyrmion. We derive an analytic formula for the skyrmion radius. The radius is controllable by the external magnetic field. It is intriguing that a skyrmion may have already been observed as a magnetic domain. A salient feature is that a single skyrmion can be created or destroyed experimentally. An analysis is made also on skyrmions in chiral magnets.

Skyrmions, originally proposed to account for baryons in nuclear physics, now play crucial roles in almost all branches of physics[1]. In condensed matter physics, in particular, the notion of skyrmion has proved to be most successful, manifesting itself in various experimental observations. Skyrmions are solitons in a nonlinear field theory characterized by the topological quantum number. In addition to its topological stability, for a soliton to materialize, the Hamiltonian must contain extra terms that introduce scale to the system. Indeed, Skyrme introduced a term of the fourth order in derivatives into his original model[2]. In an instance of quantum Hall ferromagnets, the scale of a skyrmion is determined by the competitive interplay between the Zeeman and the Coulomb interactions[3, 4]. Recently, a skyrmion lattice[5] as well as a single skyrmion[6] have been observed in chiral magnets, where the role of the Dzyaloshinskii-Moriya interaction (DMI) has been discussed[7, 8].

In this paper we propose a new mechanism of skyrmion materialization based on the magnetic dipole-dipole interaction (DDI). Magnetic DDIs exist in all magnetic materials. They introduce frustration into a ferromagnetic state. Frustration between DDIs and exchange interactions could lead to rich phenomena in magnetic materials. Indeed, the ground state of a thin ferromagnet film has a complicated magnetic domain structure comprised of stripes, bubbles or labyrinths[9–13]. We show that a giant skyrmion emerges in external magnetic field. The size of the skyrmion is so large ( $\sim 1\mu\text{m}$ ) that it may be observed simply as a magnetic domain.

We present a skyrmion spin texture in the anisotropic nonlinear sigma model. Deriving an analytic formula for the radius of a giant skyrmion, we find that there exists a minimum radius. As the magnetic field increases, the radius decreases and suddenly shrinks to zero, where a skyrmion disappears. The skyrmion spin texture would make a quantum jump to the homogeneous ground state, which breaks the conservation of the topological quantum number. Furthermore, a single skyrmion can be created by destroying the magnetic order within a tiny spot, as we soon argue. It is also pointed out that the skyrmion excitation energy becomes negative, making a formation of a skyrmion lattice possible, when the external field is less than a certain critical value. A skyrmion enjoys the topological stability, as far as the external magnetic field

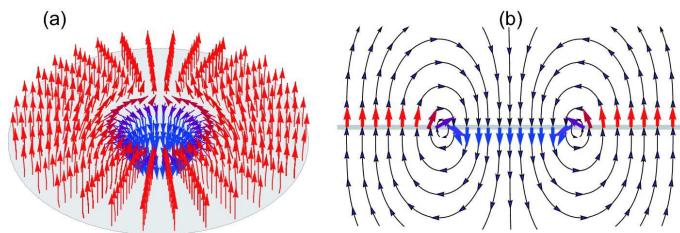


FIG. 1. (Color online) (a) Illustration of a giant skyrmion ( $\sim 1\mu\text{m}$ ) in a thin ferromagnetic film. The simplest spin texture has naturally a nontrivial Pontryagin number. It can be created by applying femtosecond optical pulse irradiation focused on a micrometer spot and thus destroying the magnetic order locally. (b) Illustration of magnetic flux lines around a skyrmion due to magnetic dipoles. When the magnetic order is destroyed locally, a new order is generated which is opposite to that of the environs, so that the magnetic flux closes by itself as short as possible.

is not too large or not too weak.

A giant skyrmion may have already been observed experimentally as a magnetic domain in a TbFeCo thin film[14]. In this experiment the ground state is a homogeneous spin-polarized state in a small external magnetic field. By applying femtosecond optical pulse irradiation focused on a micrometer spot, it is possible to destroy the magnetic order locally. Then, the DDI generates an effective magnetic field, leading to a new magnetic order with reversed magnetization inside the spot. The resultant spin texture must be that of a single skyrmion, since it is the simplest and most natural spin texture, as illustrated in Fig.1. Thus, a skyrmion can be created at any point from the ground state experimentally by destroying the magnetic order within a tiny spot. This process breaks down the continuity of the classical fields, and the conservation of the topological quantum number is lost. A giant skyrmion may also occur in chiral magnets, where the spin twists around the skyrmion so as to break the chiral symmetry, as has been illustrated in Refs.[5–7].

Our system is a two-dimensional ferromagnetic plane in perpendicular magnetic field. The basic Hamiltonian is the nonlinear O(3) sigma model  $H_J$  with easy axis anisotropy

$$H_J = \frac{1}{2}\Gamma \int d^2x [(\partial_k \mathbf{n}) \cdot (\partial_k \mathbf{n}) - \xi^{-2} (n_z)^2], \quad (1)$$

where  $\Gamma = (1/2)zS^2J$  is the exchange energy[10] ( $z$  denotes the number of nearest neighbors,  $S$  the spin per atom,  $J$  the exchange constant),  $\xi$  is the single-ion anisotropy constant, and  $\mathbf{n} = (n_x, n_y, n_z)$  is a classical field of unit length. The ground-state solutions of  $H_J$  are  $\mathbf{n} = (0, 0, \pm 1)$ .

The DDI between two spins is described by the term

$$H_D = \frac{\Omega}{4\pi} \int d^2x d^2x' \left[ \frac{\mathbf{n}(\mathbf{x}) \cdot \mathbf{n}(\mathbf{x}')}{r^3} - \frac{3[\mathbf{n}(\mathbf{x}) \cdot \mathbf{r}][\mathbf{n}(\mathbf{x}') \cdot \mathbf{r}]}{r^5} \right] \quad (2)$$

with  $\mathbf{r} = \mathbf{x} - \mathbf{x}'$  and  $r = |\mathbf{r}|$ , where  $\Omega = NS^2g^2\mu_B^2\mu_0/a^4$  is the DDI strength[10] ( $N$  denotes the number of the layers,  $g$  the Landé factor,  $\mu_B$  the Bohr magneton,  $a$  the lattice constant).

We apply the magnetic field  $h$  perpendicular to the plane,

$$H_Z = -\Delta_Z \int \frac{d^2x}{a^2} n_z(\mathbf{x}), \quad (3)$$

with the Zeeman energy  $\Delta_Z = Sg\mu_B\mu_0h$ , so that the ground state is the spin-polarized homogeneous state,  $\mathbf{n} = (0, 0, 1)$ .

The ordinary ferromagnet is described by the Hamiltonian  $H = H_J + H_D + H_Z$ . On the other hand, the chiral magnet is described by the Hamiltonian  $H = H_J + H_D + H_Z + H_{DM}$ , where

$$H_{DM} = D\mathbf{n}(\mathbf{x}) \cdot (\nabla \times \mathbf{n}(\mathbf{x})) \quad (4)$$

is the DMI term. It breaks the chiral symmetry explicitly.

The use of a continuum approximation and of classical fields to represent the spins is justified as far as we analyze phenomena whose characteristic wavelength is much larger than the lattice constant.

We first analyze the ordinary ferromagnet and then the chiral magnet. We start with the study of the ground state in weak external magnetic field. It is well known that the DDI makes the ground state to have an alternating up-down stripe-domain structure. Our results are consistent with those in literature[9–13] but we also present some new formulas. The basic object in our analysis is the one-dimensional solution of the anisotropic nonlinear sigma model (1) independent of the  $y$  coordinate. It has two types of solutions; a kink localized in the  $x$ -axis and a soliton lattice periodic in the  $x$ -axis.

The kink solution of the nonlinear sigma model (1) is given by  $n_x(x) = \sqrt{1 - \sigma^2(x)}$ ,  $n_y = 0$ ,  $n_z(x) = \sigma(x)$  with

$$\sigma(x) = \pm \tanh[(x - x_0)/\xi]. \quad (5)$$

It describes a domain wall with thickness  $\xi$  lying along the  $y$ -axis and located at  $x = x_0$ , and separates the two field configurations  $\mathbf{n} = (0, 0, 1)$  and  $\mathbf{n} = (0, 0, -1)$ . The exchange energy is  $E_{\text{kink}}^J = 2\Gamma L_y/\xi$ , where  $L_y$  is the length of the kink along the  $y$ -axis. The DDI energy (2) is found to be negative and divergent for a fixed value of  $L_y$ , indicating the ground state is a condensed phase of domain walls in the absence of the Zeeman effect.

Such a phase is described by the periodic solution,

$$\sigma(x) = \text{sn}(x/\kappa\xi, \kappa^2), \quad (6)$$

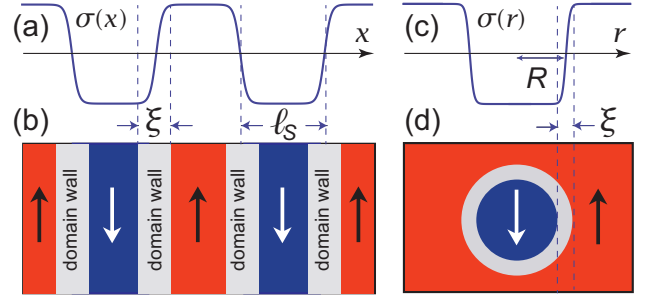


FIG. 2. (Color online) (a) Illustration of a soliton-lattice solution  $\sigma(x)$  described by the Jacobian elliptic function. (b) Illustration of the ground-state structure with an alternating up-down stripe-domains separated by domain walls. (c) Illustration of a skyrmion field configuration  $\sigma(x)$  described by (15) with (16). (d) Illustration of a skyrmion spin texture with up and down domains separated by a circular domain wall with thickness  $\xi$ .

in terms of the Jacobian elliptic function with  $0 < \kappa^2 \leq 1$ : See Fig.2(a). The periodicity of  $\sigma(x)$  is  $2\ell_S$  with

$$\ell_S \equiv 2\kappa\xi K(\kappa^2), \quad (7)$$

where  $K(\kappa^2)$  is the complete elliptic integral of the first kind. The soliton-lattice solution (6) implies that the ground state has an alternating up-down stripe-domain structure separated by domain walls, as illustrated in Fig.2(b). The width of one stripe is given by  $\ell_S$ .

Substituting (6) into the Hamiltonian (1) we obtain the energy of the soliton lattice to be

$$E_{\text{SL}}^J = \frac{\Gamma}{2\xi^2} L_x L_y \left[ \frac{2}{\kappa^2} \frac{E(\kappa^2)}{K(\kappa^2)} - \frac{1}{\kappa^2} + 1 \right] \simeq (L_x/\ell_S) E_{\text{kink}}^J, \quad (8)$$

where  $E(\kappa^2)$  is the complete elliptic integral of the second kind. The number of solitons is given by  $L_x/\ell_S$ . The last equality holds in the regime where  $\kappa \approx 1$  or  $\ell_S/\xi \gg 1$ .

We are able to estimate the DDI energy for  $\ell_S/\xi \gg 1$  as

$$E_{\text{SL}}^D = -\frac{\Omega}{2\pi} \frac{L_x L_y}{\ell_S} \ln \frac{\ell_S}{ed_F}, \quad (9)$$

where  $d_F$  is the thickness of the film. The Zeeman interaction does not make any contribution.

The total energy is

$$E_{\text{SL}} = \frac{L_x L_y}{\ell_S} \left( \frac{2\Gamma}{\xi} - \frac{\Omega}{2\pi} \ln \frac{\ell_S}{ed_F} \right). \quad (10)$$

Minimizing this with respect to  $\ell_S$ , we obtain

$$\ell_S = d_F \exp(2 + 4\pi\Gamma/\xi\Omega). \quad (11)$$

The ground-state energy is

$$E_{\text{SL}} = -(L_x L_y \Omega / 2\pi d_F e^2) e^{-4\pi\Gamma/\Omega\xi}. \quad (12)$$

The stripe-domain structure is not robust and may be deformed into a labyrinth structure. The formula (11) gives the order of the width of a stripe segment in this case.

On the other hand, in strong external magnetic field we expect the homogeneous state, which has only the Zeeman energy,  $E_{\text{hom}} = -(L_x L_y / a^2) \Delta_Z$ . By comparing this with (12), there exists the critical magnetic field  $h_c$  with the associated Zeeman energy being

$$\Delta_Z^c = (a^2 \Omega / 2\pi d_F e^2) e^{-4\pi\Gamma / \Omega\xi}. \quad (13)$$

The ferromagnet phase appears for  $\Delta_Z > \Delta_Z^c$ , or  $h > h_c$ .

We proceed to analyze a skyrmion spin texture in the ferromagnet phase. In the regime where the classical-field approximation is valid, there exists the topologically conserved charge, that is the Pontryagin number,

$$Q_{\text{sky}} = -\frac{1}{8\pi} \sum_{ij} \int d^2x \varepsilon_{ij} \mathbf{n}(\mathbf{x}) \cdot (\partial_i \mathbf{n}(\mathbf{x}) \times \partial_j \mathbf{n}(\mathbf{x})), \quad (14)$$

where  $i, j$  run over  $x, y$  with  $\varepsilon_{ij}$  being the completely anti-symmetric tensor. A spin texture possessing nonzero  $Q_{\text{sky}}$  is a skyrmion by definition.

We consider the spin texture given by

$$\begin{aligned} n_x &= -\sqrt{1 - \sigma^2(r)} \cos(\theta + \theta_0), \\ n_y &= -\sqrt{1 - \sigma^2(r)} \sin(\theta + \theta_0), \quad n_z = \sigma(r) \end{aligned} \quad (15)$$

in the cylindrical coordinate, where  $\theta_0$  is a constant parameter representing a zero-energy mode in the nonlinear sigma model  $H_J$ , while  $\sigma(r)$  is a trial function. The boundary conditions are  $\sigma(r) \rightarrow 1$  as  $r \rightarrow \infty$ , and  $\sigma(r) = -1$  at  $r = 0$ . The first condition implies this describes a soliton in the ground state with  $\sigma(r) = 1$ . The second condition is required to remove the multivalueness of the field  $\mathbf{n}(\mathbf{x})$  at the center. Substituting (15) into (14), we find that  $Q_{\text{sky}} = 1$  for any  $\theta_0$ , where the use of the boundary conditions on  $\sigma(r)$  is made. Hence, the spin texture (15) has one unit charge, and hence it is a skyrmion. Its stability is guaranteed topologically.

The chiral symmetric configuration is given by the choice of  $\theta_0 = 0$ , which minimizes the DDI energy. This is the simplest and most natural field configuration in the nonchiral magnet, as illustrated in Fig.1.

We consider a domain with radius  $R$  separated by a domain wall, where  $\sigma(r) \approx -1$  for  $r < R$  and  $\sigma(r) \approx 1$  for  $r > R$ . The wall must have thickness  $\xi$  due to the anisotropy term in (1). Such a domain structure is well described by [Fig.2(c)]

$$\sigma(r) = \tanh[(R/\xi) \log(r/R)], \quad (16)$$

which satisfies the boundary conditions at  $r = 0$  and  $r \rightarrow \infty$ . Near the domain wall, it behaves as

$$\sigma(r) = \tanh[(r - R)/\xi] \quad \text{at } r \approx R, \quad (17)$$

provided  $R \gg \xi$ , as agrees with the domain-wall solution (6).

Provided  $R \gg \xi$ ,  $\sigma(r) \approx \pm 1$  except for the domain-wall region, and the exchange energy is estimated as

$$E_{\text{sky}}^J = 4\pi\Gamma R/\xi. \quad (18)$$

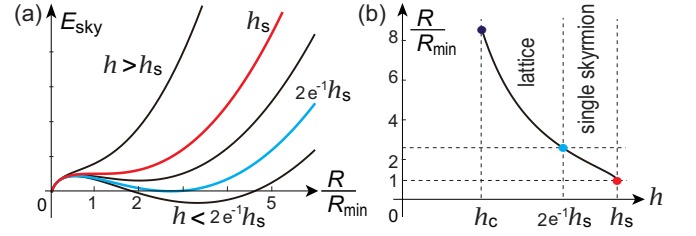


FIG. 3. (Color online) (a) The skyrmion size  $R$  is determined by minimizing the energy  $E_{\text{sky}}(R)$ . Various curves are for different magnetic field  $h$ . Skyrmion is stable only for  $h < h_s$ . (b) The skyrmion size  $R$  decreases as the field  $h$  increases. A skyrmion lattice may appear for  $h_c < h < 2e^{-1}h_s$ .

The skyrmion is not physical as it stands, though it carries the topological number, since the energy can be made zero by letting  $R \rightarrow 0$  in (18). It is made physical by the DDI in addition to the Zeeman effect, as we now show.

The DDI energy is estimated by substituting the skyrmion configuration (16) into the DDI Hamiltonian (2),

$$E_{\text{sky}}^D = -\Omega[R \ln(R/d_F) - R]. \quad (19)$$

The total excitation energy is given by

$$E_{\text{sky}}(R) = \frac{4\pi\Gamma R}{\xi} - \Omega[R \ln \frac{R}{d_F} - R] + \pi \frac{R^2}{a^2} \Delta_Z, \quad (20)$$

where the last term is the Zeeman energy. We have illustrated  $E_{\text{sky}}(R)$  for typical values of  $\Delta_Z$  in Fig.3. The variation of (20) with respect to  $R$  yields,

$$\frac{4\pi\Gamma}{\xi} - \Omega \ln \frac{R}{d_F} + \frac{2\pi\Delta_Z}{a^2} R = 0. \quad (21)$$

Solving this for  $R$  we find

$$R = -\frac{a^2 \Omega}{2\pi \Delta_Z} W_{-1} \left( \frac{\Delta_Z}{e \Delta_Z^s} \right), \quad (22)$$

where  $\Delta_Z^s = e(a^2 \Omega / 2\pi d_F e^2) \exp(-4\pi\Gamma / \Omega\xi)$ , and  $W_{-1}(z)$  is the Lambert function. We may also solve (21) for  $\Omega$ ,

$$\Omega = \frac{4\pi\Gamma/\xi + 2\pi\Delta_Z R/a^2}{\log(R/d_F)}. \quad (23)$$

This is interpreted as the formula to determine the effective DDI strength from the size of a skyrmion. A comment is in order: It follows that  $\Delta_Z^s = e\Delta_Z^c$  with (13). This is a relation peculiar to the nonchiral magnet.

The Lambert function  $W_{-1}(z)$  has a real value only for  $z > -1/e$ , as implies

$$\Delta_Z < \Delta_Z^s, \quad \text{or } h < h_s. \quad (24)$$

Namely, the skyrmion is stable only when the magnetic field is less than the critical one  $h_s$ . The minimum radius is

$$R_{\text{min}} = a^2 \Omega / (2\pi \Delta_Z^s) = \ell_S / e, \quad (25)$$

where  $\ell_S$  is the width of one stripe in the absence of the magnetic field and given by (11).

When  $h$  exceeds  $h_s$ , the radius shrinks to zero and the skyrmion disappears, which is beyond the classical-field regime of the spin. What actually happens would be that the spin direction at the skyrmion center makes a quantum jump to that of the homogeneous ground state.

The skyrmion energy is less than the ground-state energy for  $h < 2e^{-1}h_s$ , as illustrated in Fig.3. Skyrmions would condense and form a lattice to make a new ground state when the sample is cooled from high temperature in the magnetic field  $h < 2e^{-1}h_s$ . On the other hand, once a skyrmion is created in the ferromagnetic ground state ( $h > 2e^{-1}h_s$ ) and then the magnetic field is decreased at low temperature, it remains to be a stable object even for  $h < 2e^{-1}h_s$ .

We next discuss a skyrmion in chiral magnets such as MnSi and FeCoSi thin films. The Hamiltonian is given by  $H = H_J + H_D + H_Z + H_{DM}$ , where  $H_{DM}$  is the DMI term (4). The system is in the ferromagnetic phase beyond a certain critical magnetic field  $h_c$ . The skyrmion spin texture is given by (15), where the zero-energy mode  $\theta_0$  of the nonlinear sigma model  $H_J$  is fixed by minimizing the total energy. We find  $\theta_0 = -\pi/2$  due to the DMI term. Namely, the spin twists around a skyrmion as in the illustrations given in Refs.[5–7]. All the rest analysis can be carried out almost as it was. Indeed, the function  $\sigma(r)$  is given by (16). Provided  $R \gg \xi$ , the DMI energy is calculated to be

$$E_{\text{sky}}^{\text{DM}} = -2\pi DR. \quad (26)$$

There exists a small increase of the DDI energy due to the twisting of spins inside the domain wall, which we neglect. As a result the net effect is to renormalize the exchange energy as

$$\Gamma \rightarrow \Gamma_{\text{DM}} \equiv \Gamma - \frac{1}{2}\xi D \quad (27)$$

in the skyrmion excitation energy (20). Then, we can derive (21)~(25) just as they are simply by replacing  $\Gamma$  with  $\Gamma_{\text{DM}}$ . A giant skyrmion stabilized by the DDI may also occur in the chiral magnet provided  $\Gamma > \frac{1}{2}\xi D$ . The essential role of the DMI is to twist the spin texture around a skyrmion.

The present work was motivated by a recent magnetization reversal experiment[14] on a TbFeCo thin film. It is not certain if our analysis can be applicable to this material as it stands, because TbFeCo is amorphous and what is realized is a ferrimagnet. Nevertheless, it is tempting to make a comparison of our analytical results to the experimental

results by identifying the observed magnetization reversal domain as a skyrmion. Sample parameters[14, 15] are the lattice constant  $a = 0.3$  [nm], the layer thickness  $d_F = 35$  [nm] and the exchange energy  $\Gamma = 3.5 \times 10^{-20}$  [J]. The experiment was carried out in the magnetic field at 170 [Oe], where the radius of the observed skyrmion is about  $R = 1$  [ $\mu\text{m}$ ] and the thickness of the domain wall is about  $\xi = 25$  [nm]. We then use (23) to determine the effective DDI strength,  $\Omega = 8.4 \times 10^{-12}$  [J/m]. This is a good agreement with  $\Omega = 7.0 \times 10^{-12}$  [J/m] for TbFeCo, which is evaluated from its definition given below (2). We predict the minimum skyrmion radius to be  $R_{\text{min}} = 0.7$  [ $\mu\text{m}$ ]. Using these parameters, the stripe width becomes of the order of  $\ell_S = 1.9$  [ $\mu\text{m}$ ] in the absence of the magnetic field. On the other hand,  $h_s = 190$  [Oe], beyond which a skyrmion is expected to disappear.

I am deeply indebted to Y. Tokura and T. Ogasawara for illuminating discussions and for informing me as to experimental details. I am very much grateful to N. Nagaosa for fruitful discussions on the subject. This work was supported in part by Grants-in-Aid for Scientific Research from the Ministry of Education, Science, Sports and Culture No. 22740196 and 21244053.

- 
- [1] G.E. Brown and M. Rho (eds.), "The Multifaced Skyrmions", World Scientific, Singapore (2010).
  - [2] T. H. R. Skyrme, Proc. Roy. Soc. (London) A **260**, 127 (1961); Nuc. Phys. **31**, 556 (1962).
  - [3] S. L. Sondhi, *et al.* Phys. Rev. B **47**, 16419 (1993).
  - [4] M. Abolfath, *et al.* Phys. Rev. B **56**, 6795 (1997).
  - [5] Mohlbauer *et al.*, Science **323**, 915 (2009); Monzer *et al.* Phys. Rev. B **81**, 041203 (2010).
  - [6] X. Z. Yu, Y. Onose, N. Kanazawa, J. H. Park, J. H. Han, Y. Matsui, N. Nagaosa and Y. Tokura Nature, **465**, 901 (2010).
  - [7] C. Pfeleiderer and Achim Rosch, Nature **465**, 880 (2010).
  - [8] J. H. Han, J. Zang, Z. Yang, J.-H. Park and N. Nagaosa, Phys. Rev. B **82**, 094429 (2010).
  - [9] Y. Yafet and E.M. Gyogy, Phys. Rev. B, **38**, 9145 (1988).
  - [10] A.B. Kashuba and V.L. Pokrovsky, Phys. Rev. B, **48**, 10335 (1993).
  - [11] K-O. Ng and D. Vanderbilt, Phys. Rev. B, **52**, 2177 (1995).
  - [12] S.D. Bader, Rev. Mod. Phys., **78**, 1 (2006).
  - [13] O. Portmann, A. Vaterlaus and D. Pescia, Nature, **422**, 701 (2003).
  - [14] T. Ogasawara, N. Iwata, Y. Murakami, H. Okamoto and Y. Tokura, Appl. Phys. Lett. **94**, 162507 (2009).
  - [15] M. T. Rahman, *et al.* J. Appl. Phys. **97**, 10C515 (2005).